

E. Lerche, D. Van Eester, Ph. Jacquet, M.-L. Mayoral, V. Bobkov, L. Colas,  
A. Czarnecka, M. Graham, G. Matthews, I. Monakhov, R. Neu, T. Puetterich,  
F. Rimini, P. de Vries and JET EFDA contributors

# Statistical Comparison of ICRF and NBI Heating Performance in JET-ILW L-Mode Plasmas

# Statistical Comparison of ICRF and NBI Heating Performance in JET-ILW L-Mode Plasmas

E. Lerche<sup>1</sup>, D. Van Eester<sup>1</sup>, Ph. Jacquet<sup>2</sup>, M.-L. Mayoral<sup>2</sup>, V. Bobkov<sup>3</sup>, L. Colas<sup>4</sup>,  
A. Czarnecka<sup>5</sup>, M. Graham<sup>2</sup>, G. Matthews<sup>2</sup>, I. Monakhov<sup>2</sup>, R. Neu<sup>3</sup>, T. Puetterich<sup>3</sup>,  
F. Rimini<sup>2</sup>, P. de Vries<sup>6</sup> and JET EFDA contributors\*

*JET-EFDA, Culham Science Centre, OX14 3DB, Abingdon, UK*

*<sup>1</sup>Association EURATOM-Belgian State, LPP-ERM-KMS, TEC partner, Brussels, Belgium*

*<sup>2</sup>EURATOM-CCFE Fusion Association, Culham Science Centre, OX14 3DB, Abingdon, OXON, UK*

*<sup>3</sup>Max-Planck-Institut für Plasmaphysik, EURATOM-Assoziation, Garching, Germany*

*<sup>4</sup>CEA, IRFM, F-13108 Saint-Paul-Lez-Durance, France*

*<sup>5</sup>Association Euratom-IPPLM, Hery 23, 01-497 Warsaw, Poland*

*<sup>6</sup>FOM Institute DIFFER, Euratom Association, P.O. Box 1207, Nieuwegein, Netherlands*

*\* See annex of F. Romanelli et al, "Overview of JET Results",  
(24th IAEA Fusion Energy Conference, San Diego, USA (2012)).*

Preprint of Paper to be submitted for publication in Proceedings of the  
20th Topical Conference on Radio Frequency Power in Plasmas, Sorrento, Italy.

25th June 2013 - 28th June 2013

“This document is intended for publication in the open literature. It is made available on the understanding that it may not be further circulated and extracts or references may not be published prior to publication of the original when applicable, or without the consent of the Publications Officer, EFDA, Culham Science Centre, Abingdon, Oxon, OX14 3DB, UK.”

“Enquiries about Copyright and reproduction should be addressed to the Publications Officer, EFDA, Culham Science Centre, Abingdon, Oxon, OX14 3DB, UK.”

The contents of this preprint and all other JET EFDA Preprints and Conference Papers are available to view online free at [www.iop.org/Jet](http://www.iop.org/Jet). This site has full search facilities and e-mail alert options. The diagrams contained within the PDFs on this site are hyperlinked from the year 1996 onwards.



## ABSTRACT.

After the change over from the C-wall to the ITER-like Be/W wall (ILW) in JET, the radiation losses during ICRF heating have increased and are now substantially larger than those observed with NBI at the same power levels, in spite of the similar global plasma energies reached with the two heating systems. A comparison of the NBI and ICRF performances in the JET-ILW experiments, based on a statistical analysis of ~3000 L-mode discharges, will be presented.

## 1. INTRODUCTION

Neutral beam injection (NBI) and ion-cyclotron resonance heating (ICRH) are the main auxiliary heating schemes currently used in JET and will play a crucial role in allowing ITER plasmas to reach fusion relevant core temperatures. Although these heating techniques are very different by definition (NBI being based on collisional energy exchange between the high energy ions injected and the bulk plasma and ICRF relying on resonant absorption of the wave energy by the plasma species + collisional redistribution) their heating performance is, in general, comparable. One clear difference that became more evident after the change over to the new ITER-like Be/W wall (ILW) in JET [1] is the bulk impurity radiation level per MW of auxiliary power applied, which is higher during ICRF than during NBI heating [2] despite the similar global energy values reached. This is related to a higher metallic impurity content measured during ICRF operation [3] which is caused by enhanced wall / divertor sputtering due to RF sheath rectification effects [4].

Figure 1 shows a typical low triangularity L-mode discharge ( $B_0=2.65\text{T}$ ,  $I_p=2.0\text{MA}$ ) performed in JET-ILW designed to compare the ICRF and NBI heating performances. The ICRF scenario was fundamental H minority heating ( $n_H/n_e = 5\%$ ) at  $f=42\text{MHz}$  with dipole phasing and the neutral beams were injected with energies up to  $E = 125\text{keV}$ . When applying equal amounts of ICRF and NBI (a), similar global plasma energies (c) are reached but the radiated power (e) due to higher W and Ni levels (f, h) is roughly two times larger during ICRF heating. Nevertheless, the central electron temperatures (d) achieved during ICRH are considerably higher, suggesting that the impurity profiles are not peaked towards the very plasma center. This is confirmed by spectroscopic estimates of the W concentration (f), which indicate that the W profiles are hollow. However, the WI levels measured near the divertor (g) are lower during ICRH suggesting that the main source of Tungsten in this case is not in the divertor itself but is rather located in the main chamber and or upper baffles of the divertor [4,5]. The higher Ni content during ICRH (h) was also observed in the JET-C operation [6] and is related to sputtering of structures close to the ICRF antennas caused by ions accelerated in the RF sheath rectified fields. Estimates based on VUV spectroscopy associated to a coronal equilibrium model indicate that Ni is responsible for about 20-40% of the total radiation during ICRH [3], the remaining fraction being related to W [7].

## 2. STATISTICAL COMPARISON RESULTS

To better illustrate the different characteristics of ICRF and NBI heating over a larger range of plasma

parameters a database of L-mode discharges with ICRF only and NBI only heating was created. In Fig.2(a) constrained subset of this database ( $2e^{19}/m^3 < n_0 < 6e^{19}/m^3$ ,  $1.5MA < I_p < 2.5MA$ ,  $2T < B_0 < 2.8T$ ) is plotted against the total auxiliary power input. The scatter is due to several effects which were kept in the data selection: different ICRF scenarios and NBI configurations (energies, positions), different plasma shapes and gaps, different values of IP and B0, different kinetic profiles, etc. The data correspond to 0.4s time averages of the various signals and thus do not describe transient effects such as the role of sawteeth on the impurity behaviour and radiation.

Despite the large range of parameters considered, it is clear from Fig.2(a) that the overall heating performance of the two systems is comparable ( $\Delta W/\Delta P \approx 0.2MJ/MW$ ) and is similar to the one obtained with the C-wall. The radiated power (Fig.2b), which was only slightly higher during ICRH than during NBI in JET-C is now about 1.5-2 times larger, the highest values being observed in low density plasmas. As mentioned, the larger radiation observed during ICRF is due to a higher level of metallic impurities in the plasma such as W and Ni (not shown but similar trend as in Fig.1(f) and 1(g)). The fact that the W and Ni signals are strongly correlated with the ICRF power and particularly sensitive to the antenna phasing [3] suggests a close relation with RF sheath rectification effects, whose magnitude is believed not to have changed significantly with respect to the CFC wall experiments but which now, in addition to Ni, cause sputtering of W from plasma facing components [4,5]. It has to be noted that the replacement of Carbon as the main low-Z source of radiation to Beryllium lead to a decrease in the overall background radiation level [8], causing a more pronounced difference when comparing the JET-C and the JET-ILW results. Although the bulk plasma radiation being larger, the central temperatures achieved with on-axis ICRF heating are still considerably higher than the ones achieved with NBI or with off-axis heating (Fig.2c), indicating that the temperatures profiles are strongly peaked and that in these conditions the impurities are not located in the very plasma core (see [2] for the profiles' comparison). This is further illustrated in Fig.2d, which shows that the line integrated radiated power signal from a vertical bolometer detector that has a line-of-sight through the plasma centre and the divertor (core) is similar during ICRH and NBI while a more external channel crossing the plasma at mid-radius to the low-field side (edge) clearly shows a stronger contribution during ICRF heating. Soft X-ray and bolometer tomography also confirm this effect [2] and reveal that although the total impurity level is lower with NBI heating, the profiles can be strongly peaked and the local W density values near the plasma centre can exceed the ones measured during ICRH, leading to similar line integrated radiation levels in the central bolometer channels [5]. The very different impurity behaviour observed with ICRF and NBI heating is not only related to the different PWI characteristics but is also influenced by the distinct transport dynamics imposed by the different kinetic profiles and power deposition profiles inherent of each heating scheme. The influence of various effects (such as smoothing of the density gradients during NBI, increase of the temperature gradients during ICRF, the role of large sawteeth due to fast particle stabilization driven by ICRF, etc.) on impurity transport is being considered by the modelling community to explain the different impurity dynamics observed with the two heating

methods [9]. An interesting result obtained in the last JET-ILW campaign concerns the concentration of the minority H ions used for ICRF heating: It was shown that rather than using small minority concentrations (as typically used in JET-C), it can be beneficial to operate at somewhat higher levels ( $n_H/n_e \approx 15\%$ ), where the impurity content as well as the bulk radiated power are considerably lower but the heating efficiency of the fundamental H minority ICRF heating scheme, that is expected to drop at higher H concentrations [10], has not yet significantly decreased [11].

Since similar plasma energy levels per MW of auxiliary power are reached with both heating systems but the radiation fraction is considerably higher during ICRH (Fig.2e), the transport related energy confinement time defined as  $\tau_E^* = W / (P_{in} - P_{rad})$  shows a weaker degradation with power when ICRF heating is used (Fig.2(f)). For example, at  $P_{in} = 4\text{MW}$ , where the radiated fraction is  $\sim 45\%$  with ICRH, the confinement time is about 0.2s (50%) higher than with NBI. As long as it does not compromise the plasma heating performance, the higher radiation fraction observed with ICRH can be seen as favourable since in this case the transport losses through the separatrix are smaller and less power reaches the divertor and the plasma facing components. This is corroborated by IR measurements of the divertor heat loads during ICRF heated plasmas and is consistent with the lower WI levels measured at the divertor during ICRH, since the flux of energetic ions that can cause W sputtering in this region is reduced with respect to NBI heated discharges.

## SUMMARY

The analysis of a large L-mode database has shown that the ICRF and NBI heating performances are similar and have not changed significantly after the installation of the ITER-like Be/W wall. On the other hand, the radiated power during ICRF - which was only slightly higher than with NBI in the C wall - has increased considerably in JET-ILW. Although this being associated to a larger W (and Ni) level during ICRH due to enhanced material sputtering most probably caused by RF sheath effects in the main chamber, the central electron temperatures reached with on-axis ICRH are considerably higher than with NBI and the  $T_e$  profiles are strongly peaked. W spectroscopy, bolometer and soft X-ray diagnostics indicate that the impurity profiles are hollow during ICRH and that the total high-Z impurity content remains below acceptable levels in all cases and thus does not pose any problem for Lmode operation with dipole antenna phasing. Because of the higher radiated power fraction, ICRF heated plasmas feature reduced transport losses through the separatrix thus relieving the heat loads in the divertor region. The use of ICRH in high NBI power H-modes in JET-ILW to help controlling core impurity accumulation is still being assessed [12]. Although first studies indicate a positive effect of ICRH on the impurity peaking in H-mode plasmas [5], the actual demonstration that ICRF heating can help avoiding high-Z impurity accumulation in the plasma core through localized central plasma heating despite the increased edge impurity sources is still to be done in JET-ILW.

## ACKNOWLEDGMENTS

This work was supported by EURATOM and carried out within the framework of the European Fusion Development Agreement. The views expressed herein do not necessarily reflect those of the European Commission.

## REFERENCES

- [1]. G. Matthews et al., *Physica Scripta* (2011) 014001.
- [2]. M.-L. Mayoral et al., “Comparison of ICRF and NBI heated plasma performance in the JET-ILW”, this conference
- [3]. A. Czarneka et al., “Spectroscopic investigation of heavy impurity behavior during ICRH in the JET-ILW”, this conference
- [4]. V. Bobkov et al., *Journal of Nuclear Materials* **438** (2013) S160–S165.
- [5]. Ph. Jacquet et al., “ICRF heating in JET during initial operations with the ITER-like wall”, this conference
- [6]. A. Czarneka et al., *Plasma Physics and Controlled Fusion* **54** (2012) 074013.
- [7]. T. Pütterich et al., “Tungsten Screening and Impurity Control in JET”, Proc. 24th IAEA Fusion Energy Conf. (FEC2012)
- [8]. S. Brezinsek et al., *Journal of Nuclear Materials* **438** (2013) S303–S308.
- [9]. D. Kalupin et al., “Numerical analysis of JET discharges with the European Transport Simulator” subm. to *Nuclear Fusion* (2013).
- [10]. E. Lerche et al., 19th Topical Conf. on RF Power in Plasmas, Newport (USA), AIP Conf. Proc. 1406 (2011) p.245.
- [11]. D. Van. Eester et al., “Hydrogen minority ICRH in the presence of the ITER-like wall in JET”, this conference
- [12]. R. Neu et al., *Physics of Plasmas* **20** (2013) 056111

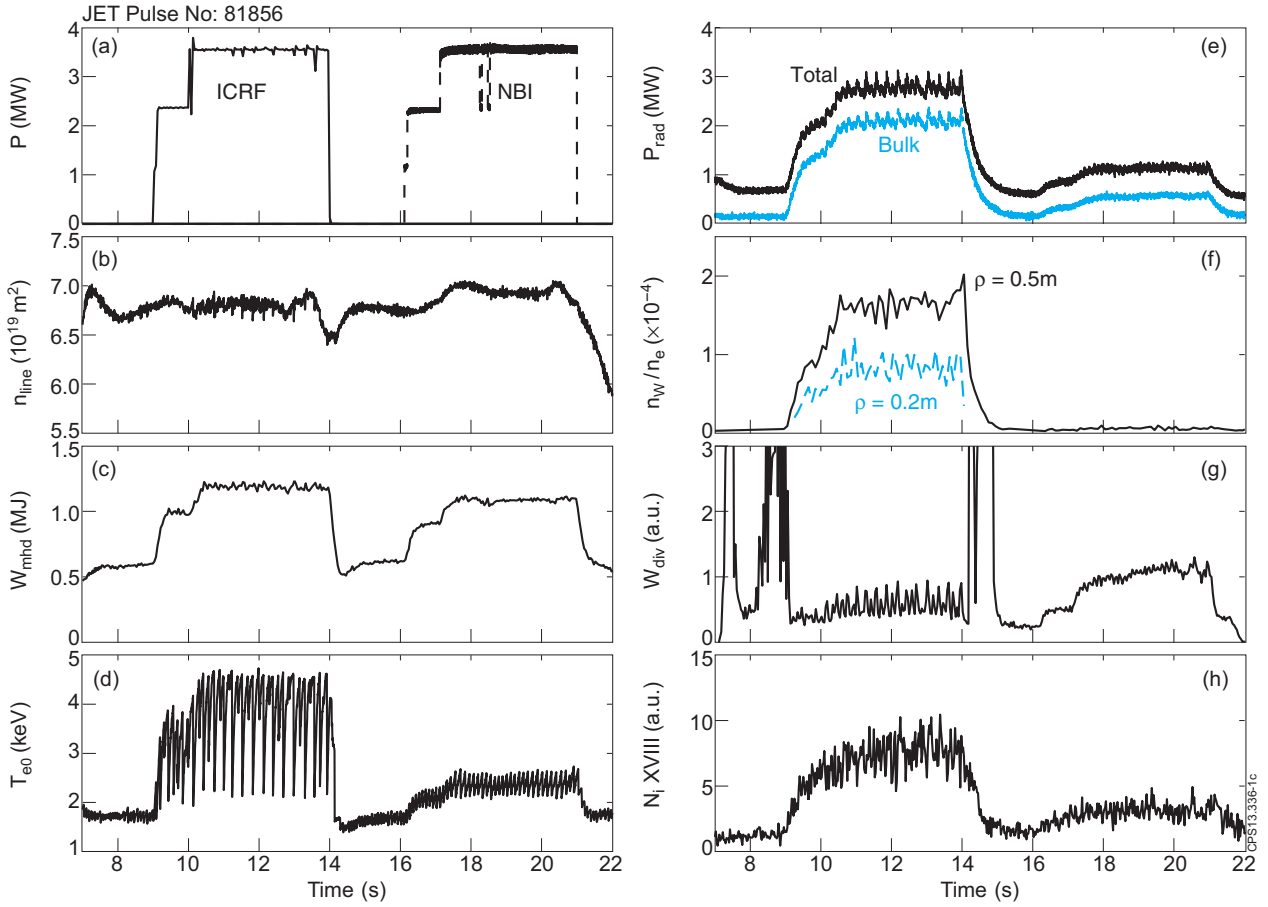


Figure 1: Time traces of (a) auxiliary power, (b) core line integrated density, (c) plasma thermal energy, (d) central electron temperature, (e) bulk and total radiated power, (f) Tungsten concentration inferred from spectroscopy at  $\rho = 0.2\text{m}$  (spectral lines) and at  $\rho = 0.5\text{m}$  (quasi-continuum), (g) W I emission from divertor spectroscopy and (h) Ni XVIII emission from VUV spectroscopy in discharge JET Pulse No: 81856.

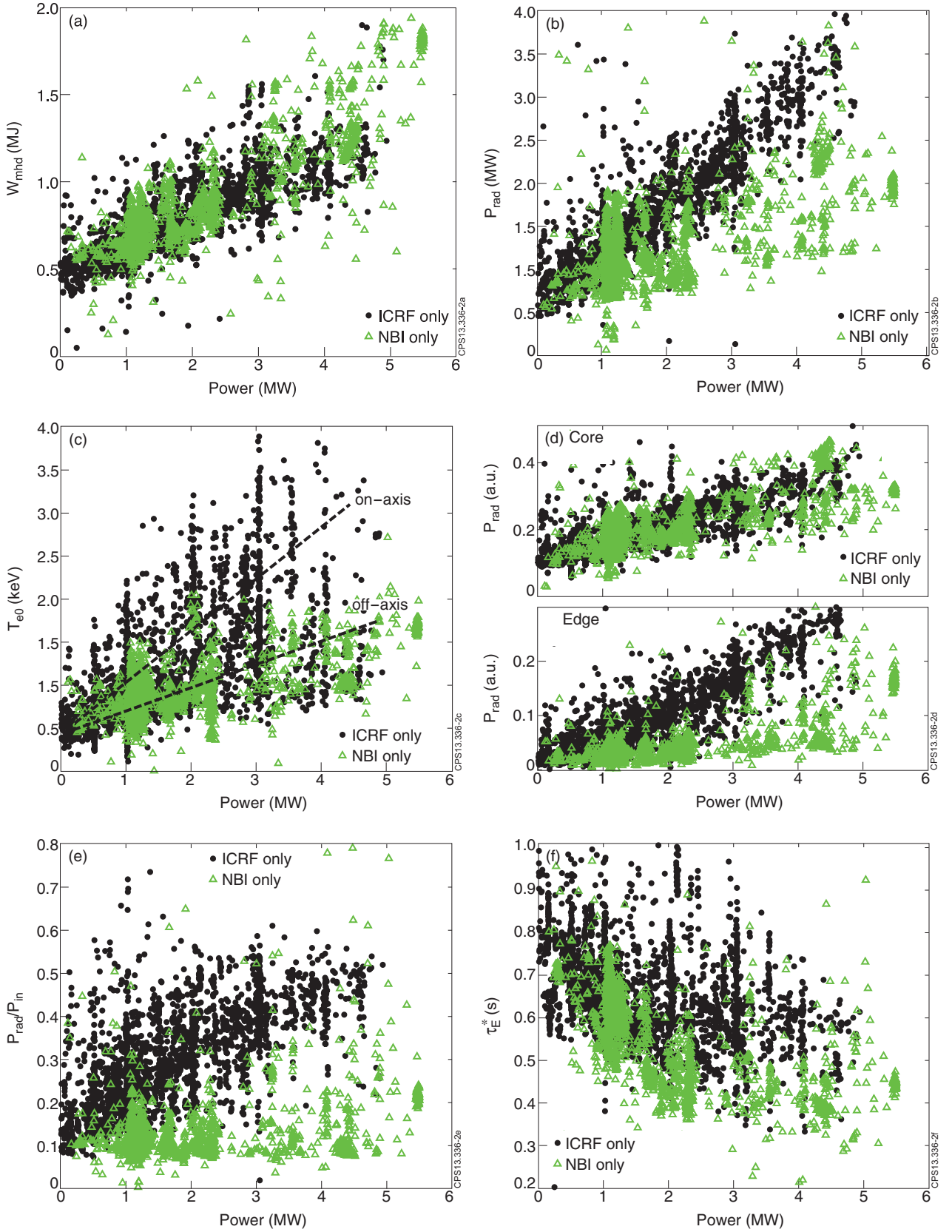


FIGURE 2: (a) Thermal plasma energy, (b) total radiated power, (c) central electron temperature, (d) line integrated bolometer signals (core and LFS edge), (e) radiated power fraction and (f) energy confinement time including radiation losses for ICRF only ( $\bullet$ ) and NBI only ( $\Delta$ ) heated discharges as function of the auxiliary power applied.